Journal of Applied Polymer Science

Waterborne polyurethane nanocomposites based on vegetable oil and microfibrillated cellulose

María Eugenia Victoria Hormaiztegui,[1] Verónica Luján Mucci,[1] Arantzazu Santamaria-Echart,[2] María Ángeles Corcuera,[2] Arantxa Eceiza,[2] Mirta Inés Aranguren[1]

[1]Instituto de Investigación en Ciencia y Tecnología de Materiales (INTEMA), UNMDP, CONICET, Facultad de Ingeniería, Av. Juan B Justo 4302, 7600 Mar del Plata, Argentina

[2]Materials+Technologies' Research Group, Department of Chemical and Environmental Engineering, Polytechnic School, University of the Basque Country, Pza. Europa 1 20018 Donostia-San Sebastián, Spain

Correspondence to: A. Eceiza (E-mail: arantxa.eceiza@ehu.eus) and M. I. Aranguren (E-mail: marangur@fi.mdp.edu.ar)

ABSTRACT: This work analyzes the differences in the final properties of two waterborne polyurethanes (WBPU) prepared with two macrodiols of different chemical structure, but similar molecular weight, as well as the variations caused by incorporating low percentages of microfibrillated cellulose nanocrystals. One of the polyurethanes was based on a synthetic but biodegradable precursor (polycaprolactone diol, PCL) and a second one based on a bio-based macrodiol derived from castor oil (CO1). The bio-based material presented higher mechanical properties at room temperature than the synthetic one, with the Young's modulus (MPa) ranging from 2.23 ± 0.09 to 84.88 ± 0.96 for the PCL and bio-based WBPUs, respectively. Additionally, the PCL-based WBPU showed to be more sensitive to the incorporation of cellulose than the bio-based WBPU, and it also suffered changes during time due to delayed crystallization. The behavior of the two systems were compared and related to the different structure of the macrodiols that led to different interfacial interactions. © 2016 Wiley Periodicals, Inc. J. Appl. Polym. Sci. **2016**, *133*, 44207.

KEYWORDS: biopolymers & renewable polymers; cellulose and other wood products; composites; polyurethanes

Received 25 February 2016; accepted 18 July 2016
DOI: 10.1002/app.44207

INTRODUCTION

Since its inception, polyurethanes (PUs) have attracted a large interest owing to its versatile properties. However, the growing consciousness regarding environmental issues has created serious concerns with respect to the use of conventional solvent borne PUs, particularly due to high volatile organic compound content. Also, increasing environmental concern and economical factors around the world have driven the efforts in the search and use of alternative raw materials in the polymer industry.[1] In particular, PUs, offering a broad variety of properties that are useful in different areas of applications, can be prepared from reactants obtained from renewable resources of wide availability.[2–4]

The behavior of PUs has been frequently related to a phase separated structure that appears in segmented PUs. In these polymers, a mixture of at least two diols, a long chain diol and a low molecular weight diol, usually referred as chain extender, are reacted with an isocyanate (functionality ≥ 2). Because of incompatibility between the long chain diol and (generally) the rest of the components, a microphase separation takes place, resulting in materials with "hard domains" or "hard segments" (HS) formed by the reacted isocyanate and chain extender and "soft domains/segments" (SS) formed by the long chain diol. To enhance this phase separation, the synthesis can be performed in two steps, with a first step in which the long chain diol is reacted with excess isocyanate and a second step in which the chain extender is incorporated and reacted. In the commercial practice, however, a single step is used for practicity reasons, resulting in more mixed phases.[5]

Moreover, a paradigm shift has been observed in the research and development of ecofriendly polymeric materials. As a result of these research efforts, waterborne polyurethane (WBPU) has emerged and grown as a sensible green alternative. The works of Dieterich *et al.* on this type of PUs are considered the first ones and the inspiration in this field.[6,7] The ability of dispersion in water of the particles of PU, results from the modification of the PU by incorporating ionic groups in its structure.[8,9]

Following the strategy of producing ecofriendly materials, the use of plant oil based diols and polyols, prepared from triglycerides or from fatty acids, in the formulation of PUs and in particular of WBPU has been addressed.[10–12] The use of plant oils

Table I. Characteristics of the Diols Used

Chemical structure	M_n	Diol
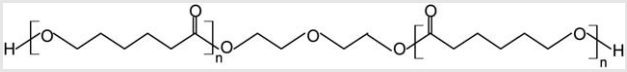	1250	PCL
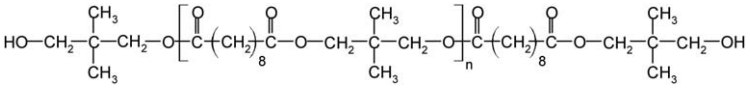	1320[a]	CO1

[a] Estimated from the chemical structure (based on NMR studies) and titration results (ASTM D 4274-05 test method A).[3]

as raw materials offers the advantages of world wide availability and competitive low price. However, the mechanical and thermal properties of bio-based PU are usually not as good as those of petroleum-based PUs, and thus different additives or modifications have been considered.[13]

Because of the good surface adhesion, low viscosity, nonflammability and easy applicability, WBPUs are used primarily as coating materials, paint additives, adhesives for various substrates, primers for metals, defoamers, associate thickeners for pigment pastes and textile dyes. However, despite of all the environmental benefits, in many instances WBPUs fail to qualify as advanced materials because of their poor mechanical performance. WBPUs are mostly thermoplastic materials with little or no gel fraction and containing a large number of hydrophilic ionic groups. Hence, they are very sensitive towards moisture and other chemical environments. This leads to inferior mechanical properties, thermal stability, and poor chemical resistance compared with the solvent-borne counterpart, restricting their use in many advanced applications.[14] The addition of nanoparticles could solve this problem, providing significant improvements in thermal and mechanical properties at very low contents of the reinforcement, while generally higher concentration of microsized reinforcements is needed to obtain the same effect.[15] In particular, the use of micro and nanoreinforcements derived from renewable resources, such as microfibrillated cellulose (MFC), cellulose and chitin nanocrystals, and bacterial cellulose, not only can improve the final properties of the synthesized composites, but also increase the amount of carbon from renewable resources in the final material.[2,16–21]

The strategy of incorporating cellulose as reinforcement of WBPU has been already applied by some authors that extracted cellulose nanocrystals (CN) from microcrystalline cellulose, flax fiber, wood (among other sources) to reinforce different WBPUs. In general, CNs display good interfacial interaction with PUs due to strong hydrogen bonding, and this is also observed in WBPU, allowing for improved dispersion of the particles. Depending on the interfacial interactions and in some cases, on their effect on phase separation, the incorporation of these particles can result in noticeable changes in the glass transition temperature of the composites.[22–24]

In this work, a single reaction step was used to prepare the PUs, and thus microphase mixing is to be expected. The use of WBPUs offers the opportunity of using the polymeric suspension as the matrix in the preparation of composites with the reinforcement dispersed in the same medium. In particular, WBPUs were synthesized from two different macrodiols, a polycaprolactone diol (PCL) and a bio-based diol consisting on sebacic acid copolymerized with 2,2-dimethylpropane-1,3-diol, selected for being both polyesters with similar molecular weights, although with different chemical structure that lead to different materials as it will be further discussed. These diols were reacted with isophorone diisocyanate (IPDI) to obtain optically clear PUs.[25] Dimethylolpropionic acid (DMPA) and triethylamine (TEA) were used to produce the ionic centers needed to formulate the aqueous PU suspensions. Since the ratios of the reactants were kept equal in both formulations, the calculated (theoretical) percentage of HSs was very similar for the two series of materials (32 and 31% for the PCL and bio based PUs). According to this, the main differences to be discussed are related to the structures of the macrodiols, their reactivity and the interactions established with the other components in the formulation, which lead to different morphologies and properties. In addition, composites based on the two WBPUs were prepared by addition of MFC, and its effect on the final properties of the composite films was analyzed. The samples were characterized by Fourier transform infrared spectroscopy (FTIR), X-ray diffraction (XRD), differential scanning calorimetry (DSC), dynamic mechanical analysis (DMA), and tensile testing. Finally, the effect of the storage time on the two different PUs was also investigated and related to their structures.

EXPERIMENTAL

Raw Materials

MFC, provided by the University of Maine, was used without modification.[26] DMPA (98% purity), IPDI (98% purity, NCO number = 24.06% determined by ASTM D2572), TEA (99% purity), dibutyltin dilaurate (DBTDL) (95% purity) and acetone were all purchased from Sigma-Aldrich Corp. and used without purification.

Bio-based WBPU were prepared from a diol derived of castor oil (CO1, OH number 85 mg KOH/g) and from PCL (used for comparison). The chemical structure and number average molecular weight (M_n) of the macrodiols are reported in Table I.

Number average molecular weight and chemical structure of the PCL diol were provided by the supplier (Sigma-Aldrich Corp.). The chemical structure and the molecular weight of the bio-

based diol were determined and previously reported by Saralegi *et al.*[3] Both macrodiols were dried under vacuum for 12 h before being used, using rotary vacuum evaporation at 60 °C.

Synthesis of WBPU

For the synthesis of the WBPU, PCL diol and DMPA (molar ratio = 1.6) were mixed under nitrogen atmosphere and heated at 85 °C until the PCL was melted. The IDPI (NCO/OH ratio = 1.4), was added dropwise and the reaction proceeded for 4 h. An amount of acetone was added to reduce viscosity and subsequently, after reducing the temperature to 60 °C, TEA was added (equimolar ratio with DMPA) to neutralize the free carboxylic acid groups in the PU chains. The product was dispersed with distilled water under vigorous stirring (800 rpm) and the remaining acetone was removed by rotary vacuum evaporation at 30 °C.[27]

On the other hand, the synthesis of bio-based diol WBPU required different reaction conditions. Temperature (100 °C), time (7 h), the use of a catalyst (1% wt DBTDL with respect to the total mass was added in the first step of the reaction) was necessary in order to obtain the bio-based diol PU, further stirring at 500 rpm during water addition.

The WBPUs obtained from PCL diol and from bio-based diol were named WBPU1 and WBPU2, respectively. From the amounts of reactants used in the formulations, the nominal percentage of HS in WBPU1 and WBPU2 were 32% and 31%, respectively.

Preparation of WBPU/MFC Composites

MFC aqueous dispersion was sonicated for 90 min in an ultrasonic bath to break possible agglomerates, 37 Hz and room temperature (Vibra-Cell 75043). Then, MFC and WBPUs were mixed using the weight ratios necessary to obtain the desired concentrations of reinforcement in the dried films (1% and 2%). The suspensions were sonicated for 30 min. The nanocomposites were prepared by casting the mixed suspensions in glass Petri dishes coated with nonstick adhesive paper at 50 °C overnight. The films were coded as WBPU#/MFCy, where y represents the weight percentage of the microfibrillar cellulose in the composite and # indicates the type of polyol used as the matrix. The nanocomposite films were stored in a desiccator for future characterization.

Characterization

FTIR Analysis. ATR-FTIR spectroscopy was performed at ambient temperature using a Nicolet Nexus spectrometer with a diamond crystal at a nominal incidence angle of 45° and ZnSe lens. The samples of the final WBPUs were cut from the films and placed on the crystal in the way of the laser. Additionally, samples taken out at different times during the reaction were also characterized by this technique. The spectra are the average of 32 scans with a resolution of 8 cm^{-1}.

Size Exclusion Chromatography. The average molecular weight and polydispersity of the WBPU were measured by size exclusion chromatography (SEC) using tetrahydrofuran as the solvent and a Thermo Scientific Ultimate 3000 equipped with a refractive index detector and calibrated with polystyrene standards (Columns: Four Phenogel GPC columns, from Phenomenex, with 5 μm particle size and 10^5, 10^3, 100, and 50 Å porosities, respectively).

Dynamic Light Scattering. The average particle size and particle size distribution of the WBPU particles in the latexes were measured by dynamic light scattering (DLS, using a BI-200SM goniometer, from Brookhaven) at 25 °C on the samples highly diluted in deionized water. The intensity of the dispersed light was determined using a source of He–Ne laser (Mini L-30, wavelength λ = 637 nm, 400 mW) and a detector (BI-APD) placed on a rotary arm which allows measuring the intensity at 90°.

Differential Scanning Calorimetry. Thermograms for the samples were obtained using differential scanning calorimetry (DSC Mettler Toledo 822^e) covering from −70 to 200 °C at 30 °C min^{-1} under N_2 atmosphere. Studies were completed using a differential scanning calorimeter DSC Pyris 1 Perkin-Elmer, covering the same range of temperature and also using N_2 atmosphere.

X-ray Diffraction. XRD measurements were conducted at a scanning speed of 0.016° s^{-1} using a X PANalytical X'Pert PRO X-ray diffractometer using Cu Kα radiation (wavelength: 1.54187 Å). The diffraction angle ranges from 2° to 60°.

The crystallite size (P_{hkl}) and interplanar distance (d_{hkl}) were calculated from the half height width of diffraction peaks at (*hkl*) plane as follows:

$$P_{hkl} = K \cdot \frac{\lambda}{\beta \cdot \cos\theta_{hkl}} \quad (1)$$

$$d_{hkl} = \frac{\lambda}{2 \cdot \sin\theta_{hkl}} \quad (2)$$

where β is a half-height width in radian of the crystalline peak, λ is the wavelength of the X-ray radiation, and *K* is the Scherrer constant taken as 0.9 according to literature.[28,29] When appropriate, the crystallinity of the samples was calculated as the ratio of crystalline area to total area.

Dynamic Mechanical Analysis. The viscoelastic properties of the recently prepared samples were measured on tensile mode with an Explexor 100 N analyzer, Gabo equipment. The experiments were carried out from −100 to 120 °C, at a scanning rate of 2 °C min^{-1} with a constant static strain of 0.05% and dynamic strain of 0.01%; and a frequency of 1 Hz, in the range of linear viscoelastic behavior.

On the other hand, the viscoelastic properties of the samples stored for one year were measured by dynamic torsion of solid rectangle bars with an Anton Paar Physica MCR 301 Rheometer. The experiments were carried out from −80 to 140 °C, at a scanning rate of 5 °C min^{-1} with a constant strain of 0.05% and a frequency of 1 Hz, in the range of linear viscoelastic behavior.

Tensile Tests. Samples for testing mechanical behavior were prepared by cutting strips from PCL-based WBPU films and composites, while dogbone specimens were cut from CO1-based WBPU films and composites. MTS equipment with a load cell of 250 N and a pneumatic grip to hold the samples was used, with a separation between the grips of 8 mm for the strips and

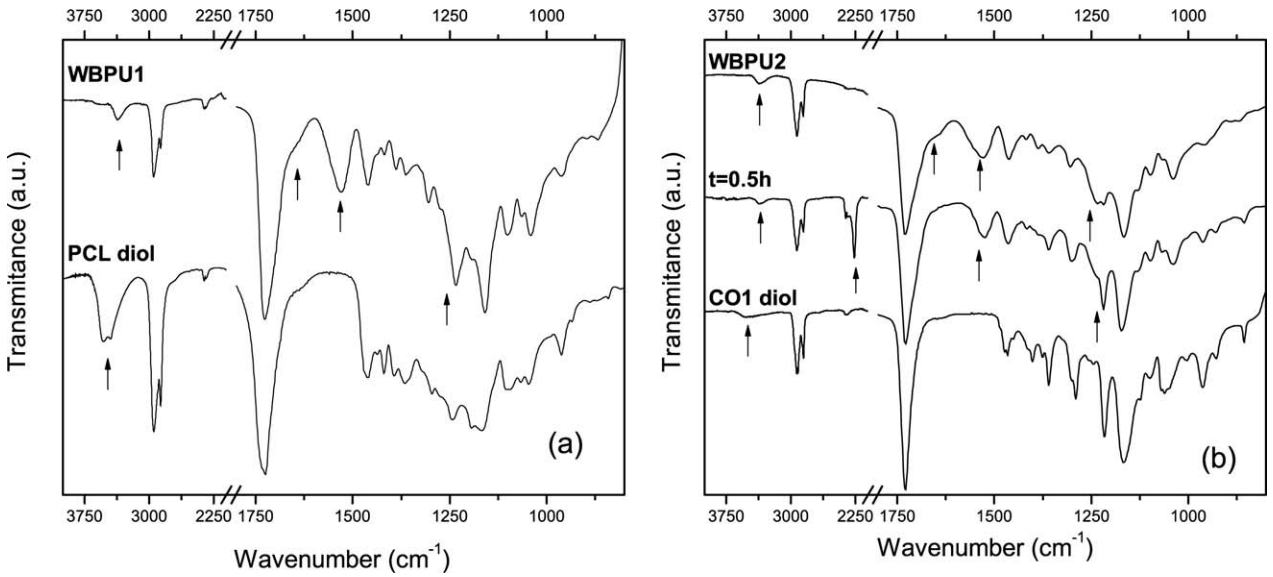

Figure 1. ATR-FTIR spectra (a) PCL diol and WBPU1 film and (b) CO1 diol, a sample taken at a reaction time, $t = 0.5$ h and the WBPU2 film.

22.5 mm for dogbone specimens. The samples had an average width of 3 mm and an average thickness of 0.39 mm for the strips and 4.94 mm and 0.37 mm, respectively for dogbone specimens. The tests were performed at a crosshead speed of 50 mm min^{-1} and the average value of at least five replicates for each sample was reported for tensile strength (σ_b), elongation at break (ϵ_b), and Young's modulus (E).

RESULTS AND DISCUSSION

Characterization of the WBPUs

The success of the synthesis was evaluated by ATR-FTIR and SEC techniques. Figure 1(a) shows the spectra of PCL and derived WBPU1 film, while Figure 1(b) shows similar information for the bio-based diol, the final WBPU2 film and a sample taken before the end of the polymerization ($t = 0.5$ h).

The intensity of the peaks at 3570 cm^{-1} and 2270 cm^{-1}, corresponding to hydroxyl and isocyanate absorptions, respectively, decrease with time as a consequence of the formation of urethane groups [intermediate spectrum is only shown for the synthesis of WBPU2 at 0.5 h, Figure 1(b)].

The final WBPUs do not show the —N═C═O group absorption band at 2270 cm^{-1} confirming the consumption of the IPDI during the formation of the PU. New bands appear, such as the band at 1260 cm^{-1}, assigned to amide-III aliphatic urethane, the amide-II band at 1535 cm^{-1}, the carbonyl stretching vibration in the amide-I region at 1630–1730 cm^{-1} and the band of the —NH stretching vibration of urethane groups at 3200–3450 cm^{-1}. The analysis of the ATR-FTIR spectra confirms the success of the polymerization reaction.[30–32] Different authors have used the absorption band of amide I to investigate the hydrogen bonding of urethane carbonyl groups.[3,17,33]

According to their observations, the peak of urethane carbonyl not involved in hydrogen bonding appears at about 1730 cm^{-1}, at 1720 cm^{-1} appears the absorption band of the hydrogen bonded carbonyl in amorphous regions and at 1685 cm^{-1} the absorption of hydrogen bonded urethane carbonyl groups that are present in ordered regions. In the PUs of this study, there is a superposition of the absorbance of carbonyl groups form the urethanes and carboxyl groups from the esters in the macrodiols appearing at 1726 cm^{-1}. The small and not well-defined shoulder that modestly appears at about 1705 cm^{-1} correspond to the hydrogen bonded carbonyl of urethane in ordered regions. The reason for the very small contribution can be related to the one step preparation and the relatively low molecular weight of the macrodiols, both characteristics that result in mixed microphases. The same observation can be made for the two different systems, although the contribution of the ordered HS appears proportionally higher in the WBPU2. The spectra of the evolution of the polymerization of WBPU2 are helpful to understand that this microphase separation occurs towards the end of the reaction, since the spectrum obtained at 0.5 h does not show any broadening of the carbonyl absorption.

XRD applied to the recently prepared samples did not offer additional information, since only the amorphous halos were observed. This behavior will be further discussed in this work, when the effect of storage is considered.

The evolution of the polymerization was followed by size exclusion chromatography (samples were taken every 60 min) until the average molecular weight was found unchanged in two subsequent measurements. Table II shows the average molecular weight and polydispersity (M_w/M_n) of WBPUs before adding TEA and water.

The WBPUs were also characterized by measuring the size of the polymer particles dispersed in water. Figure 2 and Table III

Table II. SEC Results of Polymers before the Addition of TEA and Water

Polyurethane	M_w	M_w/M_n
WBPU1	10,792	1.86
WBPU2	17,986	1.99

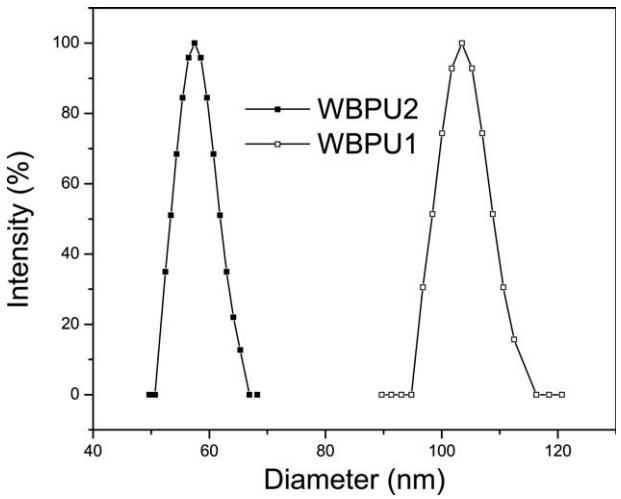

Figure 2. Particle size distribution of waterborne polyurethane dispersions WBPU1; WBPU2 measured by DLS.

show the particle size distribution and the average particle size of the two WBPU dispersions.

The different particle sizes observed in the two dispersions is probably the result of the different batch reactors used (Spain and Argentina laboratories), since it is well known that the particle sizes are much dependent on the power of the stirring applied in obtaining the dispersion.[34]

However, this is not the only possible factor, since the comparative reactivity of the specific macrodiol with respect to that of the DMPA can also affect the structure of the resulting WBPU, and the compatibility of the components in the PU, the flexibility of the macrodiol chain, the hydrophilic–hydrophobic characteristics of the two macrodiols and the free volume of the polymer structure can also be factors that can affect the size of the particles.

Despite this difference, the ranges of particle size obtained for the two formulations were acceptable for further use, according to the literature that indicate that particle sizes in the range of 20–200 nm lead to stable dispersions and can form homogeneous films.[10,35] The transparency of the films obtained was an indication of the small size and disperse distributed domains.

Characterizations of the Composites

Recently Prepared Samples. ***Thermal behavior of the composites.*** To understand the thermal behavior of the WBPUs nanocomposites, DSC scans of the different samples were analyzed and are shown in Figure 3. It can be seen that during the first heating of the recently prepared samples, the WBPU1 shows a low glass transition temperature of the soft segments (PCL), but essentially no crystallization process. On the other hand, WBPU2 shows a thermal relaxation related to the glass transition (that does not appear in a second heating), a peak due to the melting of the soft segments (CO1) that begins below room temperature and ends around 50 °C, and a relaxation at higher temperatures that is assigned to a short range order–disorder transition of the HSs.[36]

The relaxation of HSs is not observed in the DSC of WBPU1 series, which indicates that the microphases are well mixed, as it was already discussed, and this will have an important effect on the final properties of these materials.

Table IV summarizes the results of this analysis: values of T_g (determined at the mid-point of the transition), T_m and ΔH_m of the neat PUs and nanocomposites based on PCL and CO1 diols. This table also report the values of T_g measured as the temperature at which the maximum in E'' occurs.

The analysis of the results for WBPU1 and the derived MFC composites suggests that MFC acted as a nucleating agent for the crystallization of PCL in the WBPU1, which results evident by the favored soft segment crystallization, even at low concentration of the reinforcement. While no melting peak is observable in the thermograms of the neat polymer, a melting peak is present in the DSC curves of the two derived composites. Additionally, by increasing the MFC content, the crystalline phase increases, as a result of the nucleating effect of the cellulose.

DSC analysis shows that for the WBPU2 series there is not a large influence of MFC on the formation of the crystalline phase or on the glass transition of the neat PU and its composites, although in both processes a small reduction of the temperature is observed. The different thermal response of the two series of PUs is related to the different interactions between the components of the polymers. As discussed previously in the analysis of the FTIR results, microphases are mixed although, apparently a better phase separation occurred in the WBPU2. Additionally, while these results point to the existence of interactions between the PCL diol and the cellulose (that acted as a nucleation agent), they also illustrate the little interaction that occurs between the cellulose and the CO1. Probably, this is related to the more polar nature of the PCL diol, while the methyl groups that are present in CO1 and the longer $-CH_2$ sequences in this diol reduce the compatibility of the two components.

Panwiriyarat *et al.* formulated PUs from different isocyanates, including IPDI, and they concluded that separated domains of HS in these PUs are amorphous, because of the lack of symmetry of the isocyanate molecule. In their formulations, they did not change the macrodiols and extenders, but used different isocyanates and reported the crystallinity of the HS in PUs prepared from hexamethylene diisocyanate, and the amorphous nature of the HS when they used IPDI or toluene diisocyanate.[37] Thus, the DSC results obtained in the present study are in agreement with those observations: although there are partially separated domains in WBPU2, the HS are amorphous. Again, this is in agreement with the observations from XRD.

Table III. Average Particle Diameter in the WBPU Latexes

Polyurethane	Particle diameter (nm)
WBPU1	112.10 ± 0.14
WBPU2	62.17 ± 0.54

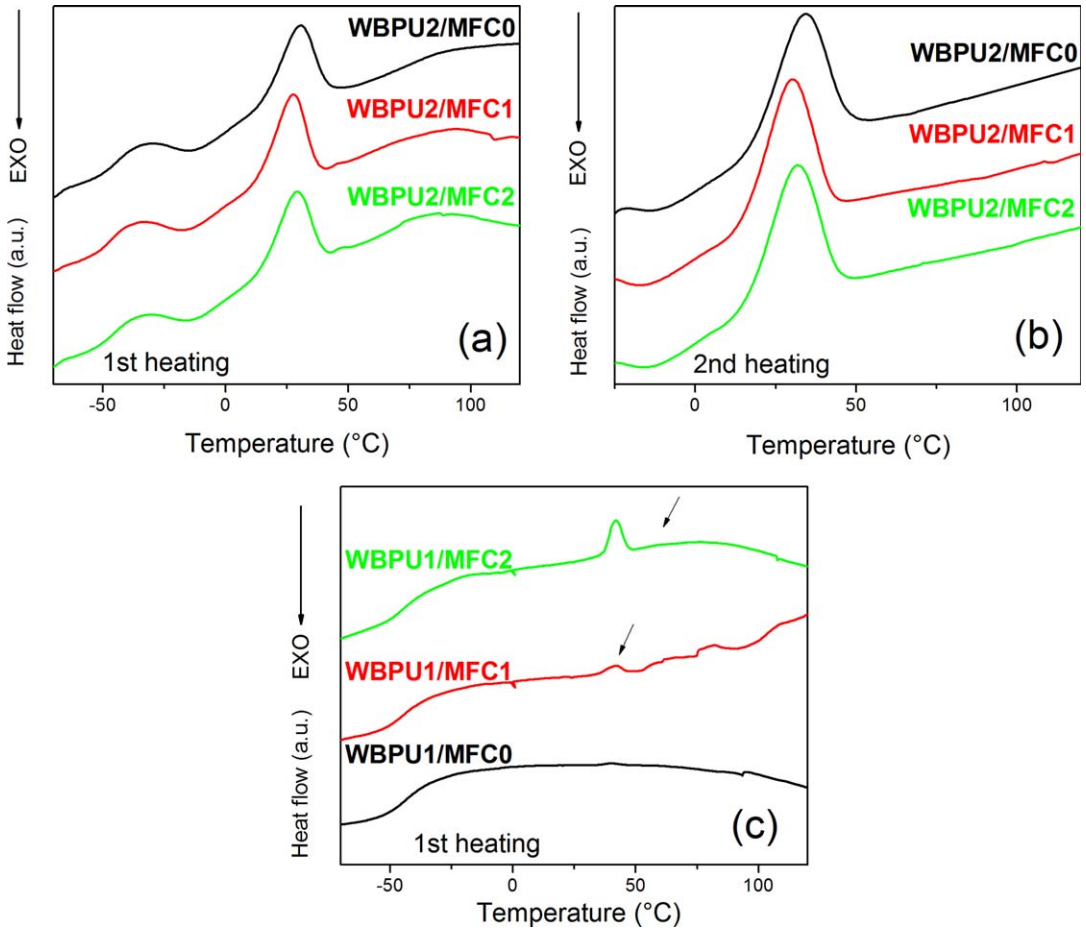

Figure 3. DSC curves of (a) 1st heating WBPU2 series, (b) 2nd heating WBPU2 series, and (c) 1st heating WBPU1 series. [Color figure can be viewed in the online issue, which is available at wileyonlinelibrary.com]

Dynamic mechanical characterization. The dynamic mechanical characterization of the samples was performed on the recently prepared samples and the results are presented in Figure 4(a,b).

The storage modulus of the unreinforced WBPU1 [Figure 4(a)] is lower than that of the WBPU2 [Figure 4(b)] in the whole range of temperatures investigated. While the value of the modulus of the WBPU2 film is about 2.5 times that of the WBPU1 film in the glassy region, it turns to be about 100 times higher at room temperature. This observation is related to the different morphologies of the two series of PUs as it has been previously discussed. Under these conditions, the WBPU1 sample is an amorphous elastomer with very low modulus. The small HS domains are mixed and dispersed in the SS. Thus, when the temperature of the test becomes higher than the glass transition temperature of the SS (T_gSS), the modulus suffers a large drop. The amorphous glassy HS slightly sustain the structure and the sample becomes a sticky liquid-like material. On the other hand, the WBPU2 film has slightly better separated microphases and the DSC has shown that it has developed a partially crystalline SS phase. Thus, the storage modulus presents higher values than the WBPU1 in this range of temperature. There is a small drop in the modulus at about 20 °C, which is believed to be the

Table IV. DSC Data of WBPUs and MFC-Derived Composites and T_g Value Analyzed from the Peak of E'' Determined by DMA Test

	$T_g$ss mid-point (°C)	$T_m$ss onset (°C)	$T_{m,}$ss peak (°C)	ΔH_mss (J g^{-1})	$T_g$ss (peak of E'') (°C)
WBPU1	−43.38	—	—	—	−38.9
WBPU1/MFC1	−44.07	37.15	41.97	0.32	−30.3
WBPU1/MFC2	−45.08	35.04	41.76	1.59	−24.1
WBPU2	−44.04	14.66	30.35	9.13	−43.2
WBPU2/MFC1	−46.56	12.41	27.36	9.55	−42.9
WBPU2/MFC2	−45.54	13.65	28.86	8.65	−43.2

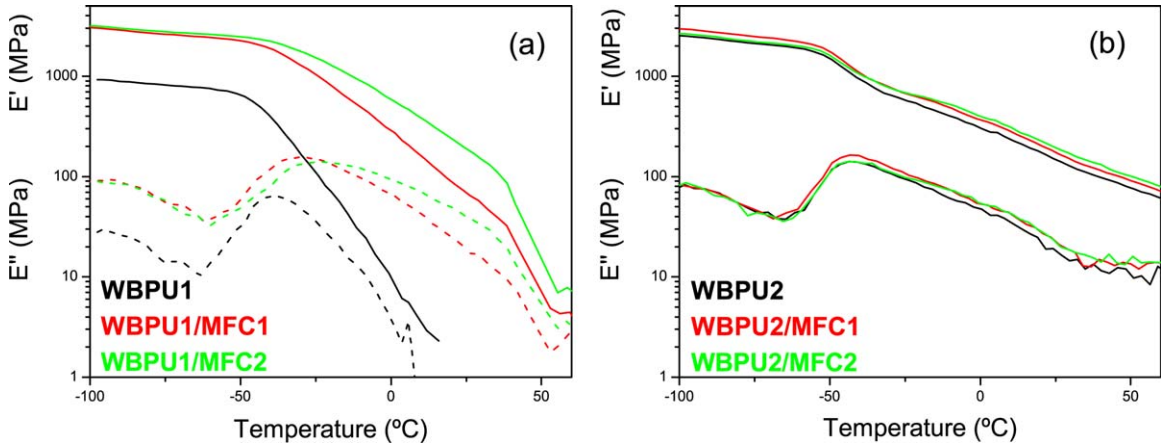

Figure 4. Storage modulus and loss modulus vs. temperature measured at 1 Hz for the neat waterborne polyurethanes and the nanocomposites (a) WBPU1 series and (b) WBPU2 series. [Color figure can be viewed in the online issue, which is available at wileyonlinelibrary.com.]

onset of the melting of SS. Since this material presents a better phase separation than WBPU1, the material maintains some cohesion due to the physical crosslinking offered by the HS.

Figure 4(a) shows that the MFC addition increased the storage modulus of the WBPU1, and widens the glass–rubber transition (analyzed from the peak of E''). By adding just 1–2 wt % of the cellulose the value of storage modulus in the WBPU1 is increased about three times in the glassy region, but the increase is larger than a 100 times at room temperature. The observed behavior is a result of the incorporation of the MFC of high modulus to the elastomeric film, but mainly (as shown by the DSC measurements) of the partial crystallization of the PCL chains in WBPU1, due to the nucleation induced by the MFC. The crystals produced in the SS, are enough to act as physical crosslinks that maintain the materials cohesion. Thus, the deep drop of modulus observed above ca. 40 °C is consequence of the melting of the mentioned crystalline phase.

On the other hand, addition of MFC to WBPU2 only improves the storage modulus in 17.2% and this can be observed in the Figure 4(b), and this is true for the whole range of temperatures considered. This is suggesting that the main contribution to the modulus in these materials is the polymer contribution. Since WBPU2 series has already developed a crystalline phase, the addition of MFC does not have much effect on the measured modulus of the WBPU2 derived composites.

Comparison of the behavior of the two series of composites suggests that the MFC interacts preferentially with the SS of the WBPU1, leading to reinforcement of the material through induced crystallization of the SS. The small change in the material is enough to give cohesion to the material; at least until the melting temperature of the soft segments is approached above room temperature. In the case of the WBPU2, the SS are less compatible with the HS, developing interactions majorly inside the given microphase. As the MFC is incorporated to the PU after the synthesis (WBPU2 dispersion), the fibers show less interaction with the polymer, and thus little variation of the properties is observed.

Mechanical properties. The results from tensile tests are summarized in Table V. A first analysis of the results shows that both PUs are elastomeric, although the WBPU2 is much stiffer than WBPU1, however still very extensible, since elongations as large as 300% can be reached.

The behavior of the two PUs is in agreement with the results analyzed from other techniques. WBPU1 is a very extensible, low modulus material because SS are not crystalline and the dispersed HSs, which are forming amorphous small domains, are maintaining the cohesion of the polymer at room temperature. On the other hand, besides the contribution of the better separated HS, WBPU2 has partially crystalline SS domains (probably of small size and well dispersed in the SS amorphous regions). This difference explains the low modulus and very high extensibility of the PCL based PU and the lower extensibility but higher modulus of the bio-based PU. The curves show, that the PUs have an initial elastic behavior, then they show some yielding and can go through strain hardening, indicating that there are HS (and SS crystals, in the case WBPU2) that act

Table V. Tensile Properties of WBPUs and Nanocomposites

	Tensile strength (MPa)	Elongation at break (%)	Young's modulus (MPa)
WBPU1	3.78 ± 0.16	1173.77 ± 77.7	2.23 ± 0.09
WBPU1/MFC1	2.21 ± 0.04	670.32 ± 27.95	4.02 ± 0.69
WBPU1/MFC2	4.04 ± 0.13	566.73 ± 8.58	8.89 ± 0.25
WBPU2	11.62 ± 0.82	330.89 ± 15.75	84.88 ± 0.96
WBPU2/MFC1	10.91 ± 1.33	302.74 ± 33.47	87.49 ± 3.49
WBPU2/MFC2	12.28 ± 0.82	292.04 ± 20.74	108.77 ± 1.95

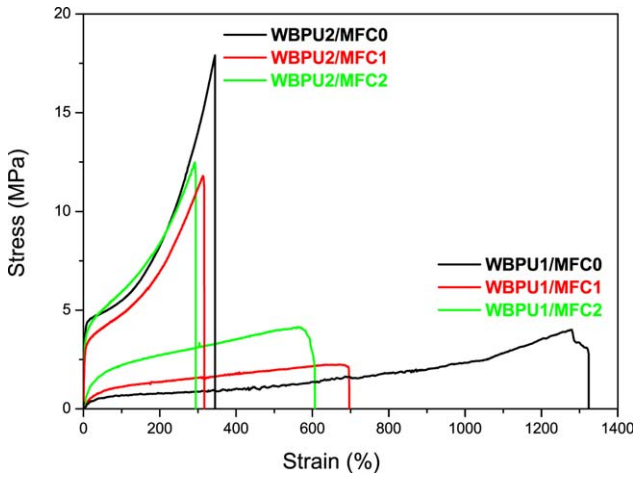

Figure 5. Tensile curves for the neat waterborne polyurethanes and the nanocomposites (a) WBPU1 series and (b) WBPU2 series. [Color figure can be viewed in the online issue, which is available at wileyonlinelibrary.com.]

as crosslinking points between the long chain diols that extend. As this extension takes place the SS chains can get ordered and new SS crystals can be formed (or chains can be oriented) that explain the strain hardening.

Moreover, the results displayed in the Figure 5 and summarized in the Table V show that the Young's modulus of the composite containing 2% MFC is four times the value of the neat WBPU1, while the elongation at break is only 48.28% of that of the neat WBPU1. As it was discussed in the DMA section, the small crystallization induced by incorporation of MFC added to the reinforcing effect of the cellulose has a very important effect on the room temperature properties. The tensile strength shows a non-monotonous trend, which may be the result of the interplay between the deleterious effect of the introduction of points of stress concentration with the addition of the MFC, and the beneficial effect of the partial crystallization of the SS and the formation of a percolating network of cellulose fibrils at concentrations as high as 2 wt %. Notice that the interplay between the SS and the MFC results in the breakage of the material before softening, followed by strain hardening, occur. Overall, these results indicate that the material becomes more rigid with the addition of the MFC.

As it could be anticipated, the mechanical tensile properties of the WBPU2 are much less affected by the addition of MFC, although the smaller changes observed follow the same trend discussed for the WBPU1 composites. This difference is related to the lower interaction fiber/matrix developed in the WBPU2 composites compared to those in the WBPU1 ones, which is explained by the greater amount of alkyl lateral short chains in the biodiol, giving it more hydrophobic character.

Clearly, the presence of MFC does not interfere with SS as it does with in the PCL composites. If any interaction develops, it probably occurs with the HS domains reducing the H-bonding in HS and thus reducing the crosslinking effect of this microphase. Then, improvement in rigidity is, majorly, the result of the higher modulus of the dispersed MFC and not of its interaction with the WBPU2 morphology.

***Thermal Degradation.*.** Figure 6 shows the TG and dTG traces of the WBPUs and derived MFC composites. The results show a clear difference between the two series of materials. WBPU1 and derived composites degrade in a single step, while WBPU2 series degrades in two steps. PU thermal degradation occurring in two steps has been reported many times in the literature and is related to the phase separated features of many PUs.[38] In the first step the degradation of the urethane groups takes place and thus, this step is related to the degradation of the HSs, isocyanate and the short diol used as chain extender. In the second step, the degradation of the macrodiol takes place, this has been proven by Panwiriyarat *et al.* that compared the temperatures of degradation of a segmented polyurethane with the thermal degradation of PUs prepared with only the macrodiol or only the short chain diol.[37] Thus, some authors have taken this result to estimate the percentage of separated phases.[38] In this study, this consideration lead to an estimation of 26% of HS in the WBPU2 (compared to the nominal of 31%), while in the case of WBPU1 and the MFC composites the phases are not separated, as it was already concluded from the different characterization techniques utilized.

Regarding to the effect of the incorporation of MFC, in the case of WBPU1 composites the interactions with cellulose shift the peak of the single degradation peak towards higher temperatures with respect to that of the neat polymer (27 °C for MFC2 and 17 °C for MFC1).

In the case of the WBPU2 composites, it is the temperature of the first peak the one more affected, while the degradation of the macrodiol suffers little change. This would indicate that the cellulose interacts with preference with the HS in this polymer, which was also observed from the tensile results of these samples.

Storage Time Effects on the WBPU Samples and Corresponding Composites. Table IV (already discussed) summarizes the results from thermograms obtained from recently prepared samples. While the overall aspect of the WBPU2 series of samples were essentially unchanged during storage (consistent with properties that did not change on time), the WBPU1 series showed increasing opacity. For this reason, samples stored for 4 months were recharacterized by DSC. Figure 7 shows the DSC curves of the neat PUs.

Figure 7(b) shows the DSC curves for the WBPU2 first heating, followed by cooling and then, a second heating. The stored WBPU2 film presented the same characteristics as the recently prepared one. Melting temperature, T_g and heat of melting suffered essentially no change during the storage. Additionally, the second heating curve repeats rather well the first heating curve, indicating that samples reached an equilibrium state rapidly.

On the other hand, as it was indicated in Table IV, no melting event appeared in the thermograms of the recently prepared WBPU1 film. However, during storage, partial crystallization at room temperature took place, what explains the increasing opacity of the samples. The chain mobility at room temperature must be certainly high for these systems, since they have very low glass transition temperature, allowing for chain rearrangement. As a result, a clear melting process appears in the DSC

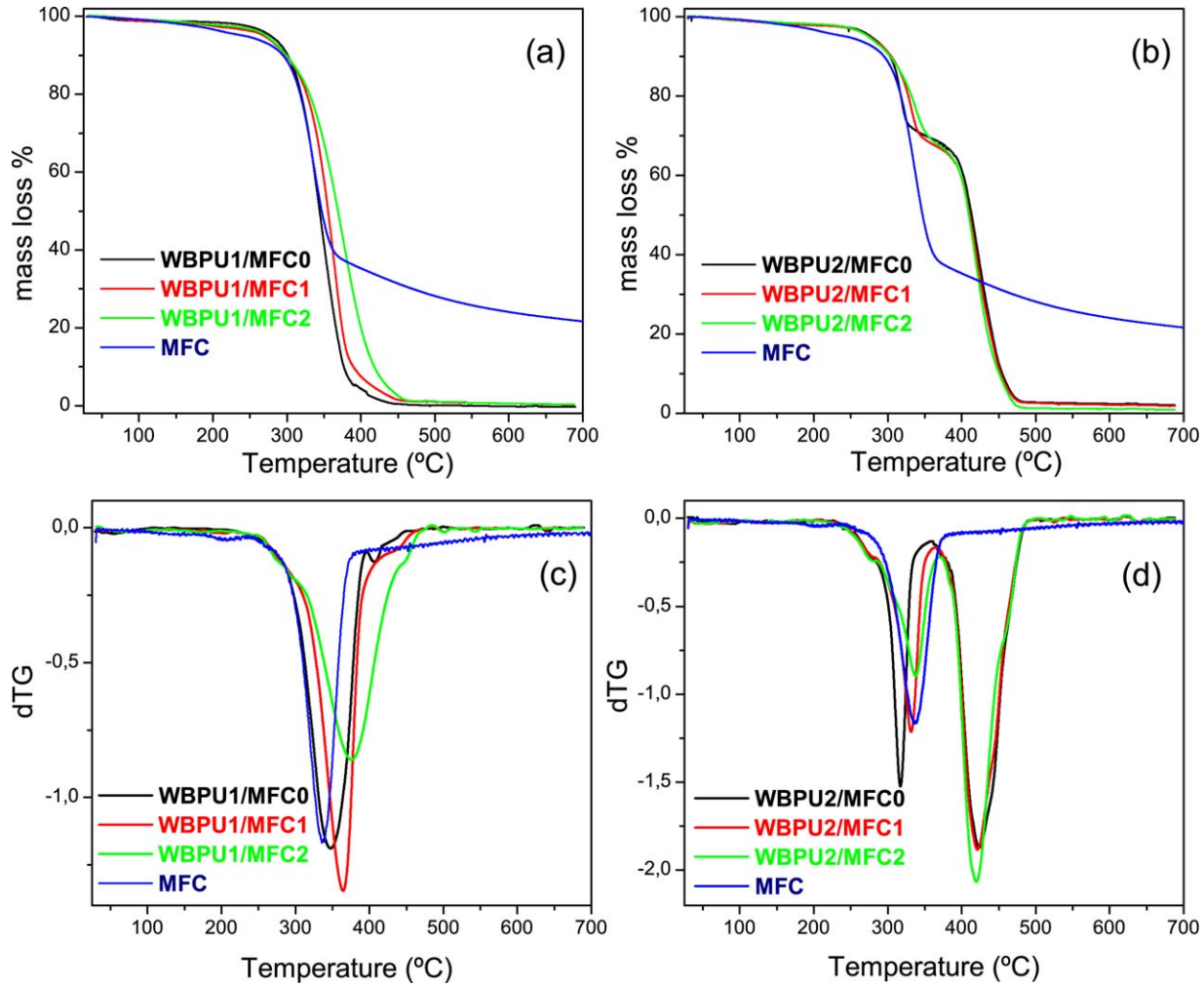

Figure 6. TG for (a) WBPU1 series, (b) WBPU2 series and dTG for, (c) WBPU1 series, and (d) WBPU2 series. [Color figure can be viewed in the online issue, which is available at wileyonlinelibrary.com.]

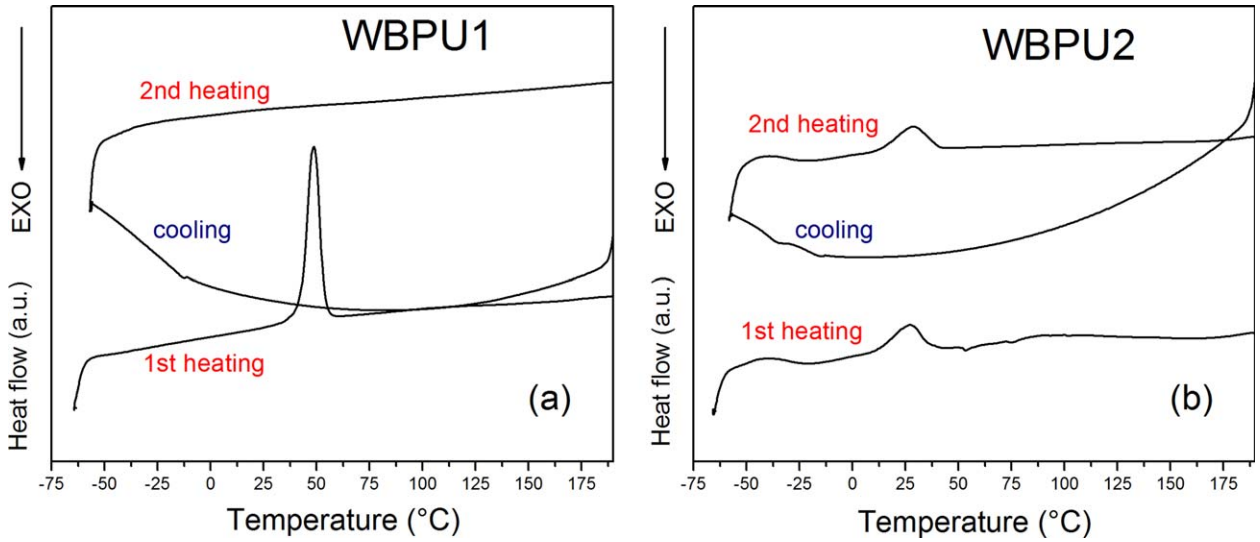

Figure 7. DSC curves (a) WBPU1 film and (b) WBPU2 film. [Color figure can be viewed in the online issue, which is available at wileyonlinelibrary.com.]

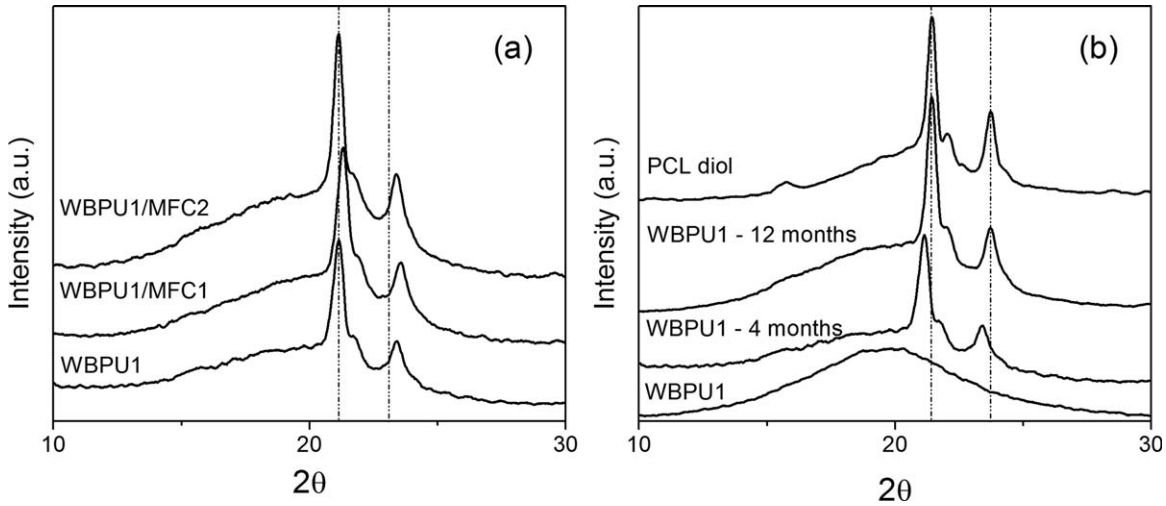

Figure 8. XRD patterns of (a) WBPU1/MFC composites and WBPU1 neat, all sample stored for 4 months and (b) increasing crystallization of PCL based polyurethane compared with PCL diol.

curve of the stored WBPU1 film. Figure 4(a) shows the first heating–cooling–second heating cycle scanned by DSC on the WBPU1 film. While melting appears very clearly in the first heating curve of the stored sample, no melting peak can be observed during the second heating part of the cycle. This indicates that much longer time is needed to produce the crystallization of the SS in this PU, in agreement with the changes observed through more extended periods of time in these samples. A similar observation on increasing "maturity" of PCL based PUs was reported by Bogdanov *et al.* who worked with PUs prepared in organic solvent and used 1,l′-methylene-bis(4-isocyanatocyclohexane) as the isocyanate component.[39]

It is also interesting to notice that while in recently prepared samples, the heat of melting increase with MFC content (ΔH_m= 0 to 1.59 J g^{-1}, for 0 to 2 wt % cellulose) due to the faster crystallization induced by the nucleation effect of the MFC, in the stored samples the heat of melting slightly decreases with the MFC content (ΔH_m = 30.196 J g^{-1} for neat WBPU1 and ΔH_m= 27.419 J g^{-1} for 2% of reinforcement). Although the dilution effect has to be considered, the reduction observed is larger than expected. This would indicate that the interactions developed between the polymer and the fibrils are favorable to the nucleation step, but can interfere in the percentage of crystallization to be reached.

To confirm that the DSC endothermic process was due to the crystallization of the PCL segments in WBPU1 series, XRD studies were performed on the samples stored for 4 months. XRD patterns of WBPU1 and the composites were shown in Figure 8(a) and confirm that all the stored samples have a crystalline phase.

The patterns exhibit the reflection peaks at 2θ = 21.14° (d = 4.203 Å) and 2θ = 23.39° (d = 3.803 Å) due to (1 1 0) and (2 0 0) planes of the PCL crystal in soft segments of the PU [interplanar distance (d_{hkl}) were calculated using eq. (2)].[29,40]

It is interesting to notice that the position of the peaks in WBPU1 composites is essentially unchanged with respect to the position in the diffractogram of the neat PU (only a minor shift towards higher angles is seen in the diffractogram of the WBPU1/MFC1, where the dispersion of the MFC should be better, and thus the consequent interactions, larger), indicating that the nature of the crystals does not change because of the addition of MFC [Figure 8(a)].

The crystallite size of the samples stored for 4 months was calculated using eq. (1) and the crystallinity of the samples was calculated as the ratio of crystalline area to total area. The crystallinity index for the WBPU1 series suffers little change with the addition of MFC (20.89% for neat WBPU, 20.09% for WBPU1/MFC1, and 18.62% for WBPU1/MFC2). The crystallite sizes were calculated using the peak at 2θ = 21.14°. Accordingly, neat WBPU has average crystals of 168.5 Å, while the crystallite size of WBPU1/MFC1 is 166.8 Å and that of WBPU1/MFC2 is 190.3 Å. Similar crystallite sizes have been reported by Sahoo *et al.* who work with a PU block copolymer obtained with PCL, MDI and 1,4-butanediol by a two-step process, with 30 wt % of hard-segment content (e.g., neat PU 133 Å).[29]

XRD patterns of PCL diol and samples of WBPU1 stored for different length of times are shown in Figure 8(b). Comparison of the XRD patterns confirm that the crystalline phase correspond to the PCL segments (2θ = 21.14° and 2θ = 23.39°) and that the crystallinity of the samples increases with time. It can also be noticed that the positions of the peaks slightly shift during storage, to become coincident with the position observed in the XRD of the PCL diol at 12 months, which supports the evolution of the microphase separation during storage.

The changes observed in the WBPU1 series of materials are expected to have an important influence in the properties of the films. Thus, it is important to be aware of these potential changes in PCL derived samples and indicate the conditions of the testing.

Figure 9 shows the comparison of the dynamic oscillation tests performed on the recently prepared samples and the samples stored for one year. It must be noticed that a tensile DMA was

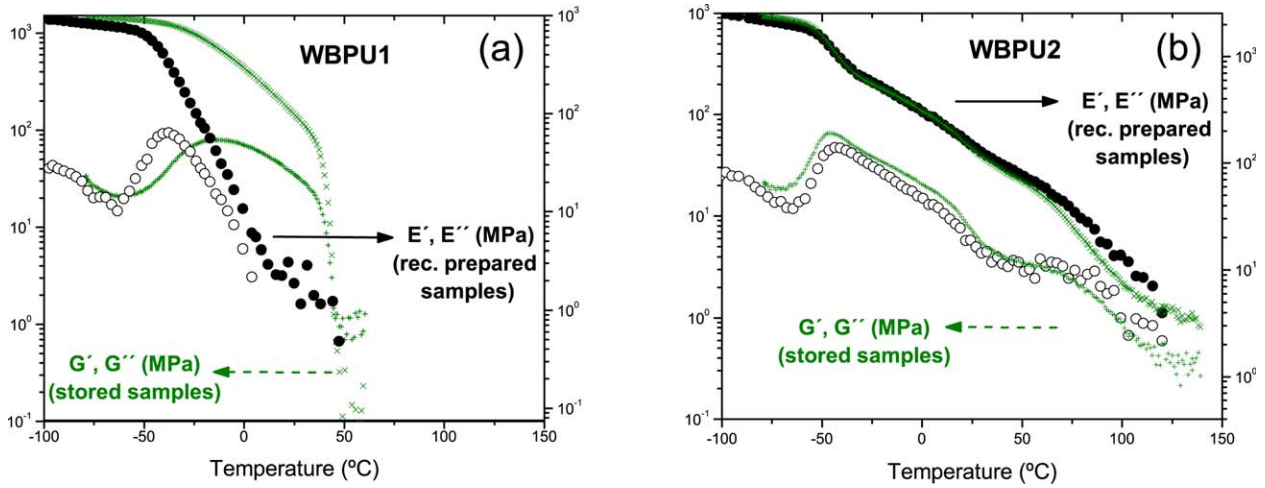

Figure 9. Storage modulus and loss modulus vs. temperature (a) WBPU1 neat recently prepared samples (E', E'') and WBPU1 stored for 12 months (G', G''), (b) WBPU2 neat recently prepared samples (E', E'') and WBPU2 stored for 12 months (G', G'').[Color figure can be viewed in the online issue, which is available at wileyonlinelibrary.com.]

used in the characterization of the recently prepared samples and a torsion rheometer (bar fixture) was used for the stored samples, as a consequence of this being a collaborative effort between two different laboratories. In spite of the use of two different equipments and related, but different dynamic properties measured, the shape of the curves and transitions show excellent correlation.

Figure 9(a) shows that the T_g of SS in WBPU1 increased as a result of the PCL crystals that were formed in the bulk of the SS domain during storage, thus reducing the mobility of amorphous chains. Additionally, the storage modulus decreases more slowly than it does in the recently prepared sample, right up to the point where the SS chains melt, and then it rapidly drops, because the material flows.

The WBPU2 samples show almost no change during storage, although the drop in both moduli due to SS melting is more clear, which could just be a result of the different equipments used in the measurement or it could also indicate that phase separation may have progressed (although at a very small degree) in this sample too.

CONCLUSIONS

In this work, a biodiol based on castor oil was used in the synthesis of a WBPU, and its characteristics and behavior were compared with a WBPU based on a PCL, both with similar nominal HS content.

The use of the biodiol allowed synthesizing stiffer elastomeric WBPU materials than those derived from PCL, but still with high extensibility. The Young's modulus of the PUs cover a wide range from 2.23 ± 0.09 MPa to 84.88 ± 0.96 MPa for the PCL and bio-based WBPUs, respectively. The behavior of the films, including their thermal degradation, was shown to depend on the chemical structure of the diol and the polymer capability to crystallize.

In the composites, the addition of MFC has a remarkable effect on WBPU1, increasing its mechanical properties and acting as a nucleating agent for the crystallization of the PCL segments. It was confirmed that the PCL segments in the WBPU1 materials continue crystallizing during storage, changing largely the thermal and dynamic mechanical properties of the films.

Otherwise, the addition of MFC to WBPU2, has a comparative lower effect on the final properties of the materials. This polymer rapidly develops a crystalline phase, so that the effect of the addition of MFC is not as dramatic as in WBPU1. Additionally, the properties do not change with time, which is considered an advantage for the use of this material.

ACKNOWLEDGMENTS

The researchers from Argentina thank CONICET, MINCyT, and UNMdP for their financial support. The researchers from Spain thank the Basque Government (IT-776-13) and Spanish Ministry of Economy and Competitiveness (MINECO) (MAT2013-43076R) for their financial support.

All the authors acknowledge the financial support of the project "Bio-based polyurethane composites with natural fillers (BIOPURFIL)," of the European Union within Marie Curie Action program (PIRSES-2012-318996). Additionally, technical support provided by General Research Services (SGIker) from the University of the Basque Country is gratefully acknowledged, as well as the technical support of Mr. Oscar Casemayor from the Polymer Characterization Laboratories in INTEMA (Argentina).

REFERENCES

1. Gogoi, S.; Karak, N. *Polym. Adv. Technol.* **2015**, *26*, 589.
2. Lin, S.; Huang, J.; Chan, P. R.; Wei, S.; Xu, Y.; Zhang, Q. *Carbohydr. Polym.* **2013**, *95*, 91.
3. Saralegi, A.; Rueda, L.; Fernández-d'Arlas, B.; Mondragon, I.; Eceiza, A.; Corcuera, M. A. *Polym. Int.* **2013**, *62*, 106.
4. Wik, V. M.; Aranguren, M. I.; Mosiewicki, M. A. *Polym. Eng. Sci.* **2011**, *51*, 1389.

5. Ionescu, M. Rapra Handbook: Chemistry and Technology of Polyols for Polyurethanes; Rapra Technology: Shropshire, UK, **2005**; pp 1–44.
6. Dieterich, D.; Keberle, W.; Wuest, R. J. *J. Oil Col. Chem. Assoc.* **1970**, *53*, 363.
7. Dieterich, D. *Prog. Org. Coat.* **1981**, *9*, 281.
8. Formo, M. W.; Jungermann, E.; Norris, F. A.; Sonntag, N. O. V. Bailey's Industrial Oil and Fat Products; John Wiley & Sons: New York, **1985**; Vol. *1*, 4th ed., pp 453.
9. Guo, Y.; Guo, J.; Li, S.; Li, X.; Wang, G.; Huang, Z. *Colloids Surf. A Physicochem. Eng. Asp.* **2013**, *427*, 53.
10. Madbouly, S. A.; Xia, Y.; Kessler, M. R. *Macromolecules* **2013**, *46*, 4606.
11. Petrović, Z. S. *Contemp. Mater.* **2010**, *I*(1), 39.
12. Fu, C.; Hu, X.; Yang, Z.; Shen, L.; Zheng, Z. *Prog. Org. Coat.* **2015**, *84*, 18.
13. Park, S.; Oh, K.; Kim, S. *Compos. Sci. Technol.* **2013**, *86*, 82.
14. Gogoi, S.; Karak, N. *ACS Sustainable Chem. Eng.* **2014**, *2*, 2730.
15. Cao, X.; Habibi, Y.; Lucia, L. *J. Mater. Chem.* **2009**, *19*, 7137.
16. Dai, L.; Long, Z.; Ren, X.; Deng, H.; He, H.; Liu, W. *J. Appl. Polym. Sci.* **2014**, *41051*, 1.
17. Huang, J.; Zou, J. W.; Chang, P. R.; Yu, J. H.; Dufresne, A. *Express Polym. Lett.* **2011**, *5*, 362.
18. Saralegi, A.; Gonzalez, M.; Valea, A.; Eceiza, A.; Corcuera, M. A. *Compos. Sci. Technol.* **2014**, *92*, 27.
19. Veigel, S.; Grüll, G.; Pinkl, S.; Obersriebnig, M.; Müller, U.; Gindl-Altmutter, W. *React. Funct. Polym.* **2014**, *85*, 214.
20. Wang, Y.; Tian, H.; Zhang, L. *Carbohydr. Polym.* **2010**, *80*, 665.
21. Zou, J.; Zhang, F.; Huang, J.; Chang, P. R.; Su, Z.; Yu, J. *Carbohydr. Polym.* **2011**, *85*, 824.
22. Yao, X.; Qi, X.; He, Y.; Tan, D.; Chen, F.; Fu, Q. *ACS Appl. Mater. Interfaces* **2014**, *6*, 2497.
23. Gao, Z.; Peng, J.; Zhong, T.; Sun, J.; Wang, X.; Yue, C. *Carbohydr. Polym.* **2012**, *87*, 2068.
24. Liu, H.; Cui, S.; Shang, S.; Wang, D.; Song, J. *Carbohydr. Polym.* **2013**, *96*, 510.
25. Polus, I. *Eur. J. Wood Wood Prod.* **2003**, *61* (3), 238.
26. Kumar, V.; Bollström, R.; Yang, A.; Chen, Q.; Chen, G.; Salminen, P.; Bousfield, D.; Toivakka, M. *Cellulose* **2014**, *21*, 3443.
27. Cao, X.; Dong, H.; Li, C. M. *Biomacromolecules* **2007**, *8*, 899.
28. Cullity, B. D.; Stock, S. R. Elements of X-ray Diffraction; Prentice-Hall Inc.: New Jersey, **2001**; 3rd ed., Chapter 5, pp 170–184.
29. Sahoo, N. G.; Jung, Y. C.; Yoo, H. J.; Cho, J. W. *Macromol. Chem. Phys.* **2006**, *207*, 1773.
30. Cakić, S. M.; Spírková, M.; Ristić, I. S.; Jaroslava, K.; Budinski-Simendić, J. K.; Cincović, M. M.; Poreba, R. *Mater. Chem. Phys.* **2013**, *138*, 277.
31. García-Pacios, V.; Costa, V.; Colera, M.; Martín-Martínez, J. M. *Int. J. Adhes. Adhes.* **2010**, *30*, 456.
32. Pérez-Limiñana, M. A.; Arán-Aís, F.; Torró-Palau, A. M.; Orgilés-Barcel, C.; Martín-Martínez, J. M. *Int. J. Adhes. Adhes.* **2005**, *25*, 507.
33. Gao, Z.; Peng, J.; Zhong, T.; Sun, J.; Wang, X.; Yue, C. *Carbohydr. Polym.* **2012**, *87*, 2068.
34. Wicks, Z. W.; Jr.; Wicks, D. A.; Rosthauser, J. W. *Prog. Org. Coat.* **2002**, *44*, 161.
35. Steward, P. A.; Hearn, J.; Wilkinson, M. C. *Adv. Colloid. Interface* **2000**, *86*, 195.
36. Fang, C.; Zhou, X.; Yu, Q.; Liu, S.; Guo, D.; Yu, R.; Hu, J. *Prog. Org. Coat.* **2014**, *77*, 61.
37. Panwiriyarat, W.; Tanrattanakul, V.; Pilard, J. F.; Pasetto, P.; Khaokong, C. *J. Appl. Polym. Sci.* **2013**, *130*, 453.
38. Cervantes-Uc, J. M.; Moo Espinosa, J. I.; Cauich-Rodríguez, J. V.; Ávila-Ortega, A.; Vázquez-Torres, H.; Marcos-Fernández, A.; San Román, J. *Polym. Degrad. Stab.* **2009**, *94*, 1666.
39. Bogdanov, B.; Toncheva, V.; Schacht, E. *J. Therm. Anal. Calorim.* **1999**, *56*, 1115.
40. Thakur, S.; Karak, N. *Prog. Org. Coat.* **2013**, *76*, 157.